Journal of Materials Chemistry

Cite this: J. Mater. Chem., 2011, 21, 3226

www.rsc.org/materials

PAPER

Synthesis and applications of difluorobenzothiadiazole based conjugated polymers for organic photovoltaics†

Zhao Li,*[a] Jianping Lu,[b] Shing-Chi Tse,[b] Jiayun Zhou,[b] Xiaomei Du,[a] Ye Tao[b] and Jianfu Ding*[a]

Received 30th November 2010, Accepted 7th January 2011
DOI: 10.1039/c0jm04166a

A new electron deficient building block, difluorobenzothiadiazole (FBT) was designed and synthesized for the first time. Two low band gap polymers containing this unit or benzothiadiazole (BT) and an electron rich unit, benzo[1,2-b:4,5-b′]dithiophene (BDT) were synthesized by Stille coupling reaction. It was found that fluorine substitution significantly lowered the energy levels but did not affect the UV absorption properties of the polymer. Comparatively, the fluorinated polymer showed a higher melting point and a reduced solubility. The electrical and photovoltaic properties of these polymers were studied by fabricating thin film transistors and polymer solar cells. The solar cell based on FBT polymer and $PC_{71}BM$ gives power conversion efficiency up to 3.4% under AM 1.5 G illumination (100 mW cm^{-2}).

1. Introduction

Compared with inorganic silicon based solar cells, organic solar cells show huge commercial potentials for flexible and large area applications, because the devices could be manufactured by existing low-cost industrial technology, such as ink-jet and roll to roll printing. Another important advantage of organic solar cells is the diversity of the molecular structures in organic chemistry, where numerous combinations of various building blocks are available. So the properties of the resulting materials, such as solubility, charge mobility and energy levels for photovoltaic applications can be easily tuned.[1]

Up to now, the most efficient and commonly used architecture for the active layer of organic solar cells is the bulk heterojunction (BHJ) structure of two components:[2] a conducting polymer as an electron donor and a fullerene derivative as an electron acceptor. For the conducting polymers, several crucial properties are required to achieve a highly efficient solar cell.[1] First, it should have a good solubility and can be easily fabricated into a thin film from solution. Second, the polymer should show high absorption toward sun light since fullerene derivatives only has very limited absorption in the solar spectrum. Third, the polymer should have a good hole mobility, at least comparable to the electron mobility of fullerene derivatives, so the separated charge carrier can be easily transported to the corresponding electrodes. Forth, the energy levels of this polymer should match with fullerene to facilitate efficient exciton separation and charge transfer.

To satisfy these requirements, people usually build alternating copolymers comprised of electron rich and electron deficient units. On one hand, such a structure can induce intra-chain charge transfer and dramatically lower the band gap of resulting polymers. So the polymers often show strong absorption in the visible region. On the other hand, their highest occupied molecular orbital (HOMO) and lowest unoccupied molecular orbital (LUMO) energy levels can be easily adjusted by choosing different combinations of electron rich and deficient units. Among the vast variety of the developed electron deficient blocks, 2,1,3-benzothiadiazole (BT) has attracted much research attentions, and has been copolymerized with many electron rich units, such as fluorene,[3] 4H-cyclopenta[2,1-b;3,4-b′]dithiophene,[4] carbazole,[5] benzo[1,2-b:4,5-b′]dithiophene (BDT),[6] dithieno[3,2-b:2′,3′-d]pyrrole,[7] dithienosilole,[8] indolo[3,2-b]carbazole,[9] and indenofluorene *etc.*[10] High performance solar cell devices with power conversion efficiency (PCE) over 5% have been reported by several groups based on these materials.[4,8,11] Furthermore, the 5 and 6 positions of BT are available to attach with a functional group to modify properties of the final polymers. For example, Bo *etc.* introduced two alkyloxy chains there to improve the solubility of the resulting polymers.[12] Yamashita *etc.* fused other electron deficient rings to these positions to obtain [1,2,5]thiadiazolo[3,4-g]quinoxaline and benzo[1,2-c;3,4-c′]bis[1,2,5]thiadiazole,[13] which demonstrated very strong electron withdrawing capability and resulted in ultra-small band gap polymers.[14]

In this work, we attempted to introduce two fluorine atoms onto these two positions to produce a new electron deficient unit, 4,7-di(thien-2-yl)-5,6-difluoro-2,1,3-benzothiadiazole (FBT). This unit was then copolymerized with an electron rich BDT unit

[a]*Institute for Chemical Process and Environmental Technology (ICPET), National Research Council of Canada (NRC), 1200 Montreal Road, Ottawa, ON, Canada K1A 0R6. E-mail: zhao.li@nrc-cnrc.gc.ca; jianfu.ding@nrc-cnrc.gc.ca*
[b]*Institute for Microstructural Sciences (IMS), National Research Council of Canada (NRC), 1200 Montreal Road, Ottawa, ON, Canada K1A 0R6*
† NRC Publication Number: NRCC 52825.

to afford a new copolymer, poly(4,8-di(3-pentyl-undecyl)benzo[1,2-b:4,5-b′]dithiophene-alt-4,7-bis(4-octyl-2-thienyl)-5,6-difluoro-2,1,3-benzothiadiazole) (**P2**). For comparison, its non-fluorinated counterpart, poly(4,8-di(3-pentyl-undecyl)benzo-[1,2-b:4,5-b′]dithiophene-alt-4,7-bis(4-octyl-2-thienyl)-2,1,3-benzothiadiazole) (**P1**) was also prepared. Their optical, electrochemical, thermal properties, and their devices performance in thin film transistors (TFT) and BHJ solar cells have been characterized. We demonstrated that the fluorine substitution did not change the UV absorption but pushed down the HOMO energy level, thus improved the environmental stability of corresponding polymer. The organic solar cells based on FBT polymer also showed a higher power conversion efficiency (PCE) than BT polymer.

2. Results and discussion

2.1. Material design and synthesis

Fluorinated conjugated polymers show very interesting features.[15] Fluorine atoms can lower both the HOMO and LUMO energy levels, so the materials will display a greater resistance against the degradative oxidation. A lower HOMO energy level also means a higher open circuit voltage (V_{oc}) for polymer solar cells since V_{oc} is usually determined by the difference between the HOMO of the polymer and the LUMO of the fullerene derivative.[16] These features are highly desired in polymer materials for photovoltaic applications. Indeed, high V_{oc} and very high PCE were obtained by introducing fluorine into organic photovoltaic polymers very recently.[17]

Based on the well studied BT structure, we designed and synthesized fluorinated BT as shown in Scheme 1. This synthesis started from nitration of 1,4-dibromo-2,3-difluorobenzene, which was prepared using a reported two-step reaction in a high yield (90%).[18] The crude product can be purified by column chromatograph to give a pure product **1** in a moderate yield (31%), which was then reacted with 2-tributyl stannyl-4-octyl thiophene to give compound **2** by palladium catalyzed Stille coupling reaction. Two nitro groups on **2** were reduced to diamine **3** using iron powder in acetic acid solution. Heterocycle **4** was prepared in 94% yield by reacting diamine **3** with N-thionylaniline and trimethylsilyl chloride in pyridine at 80 °C.[19] Dibromo-monomer **5** was obtained by bromination of **4** with NBS in chloroform using silica gel as catalyst. We introduced octyl side chains on each thiophene unit to improve the solubility of the resulting polymers.[9,20]

Recently, benzo[1,2-b:4,5-b′]dithiophene (BDT) based polymers have shown very promising properties in organic electronic devices, especially in polymer solar cells.[17,21] During the preparation of this manuscript, You *etc.* reported a BDT based polymer with branched alkyl groups at the 4- and 8- position of BDT.[22] However, detailed synthetic procedure, especially the synthesis of the key starting compound (branched alkyl chain substituted acetylene) was not reported. We independently synthesized a similar BDT monomer and the procedure is shown in Scheme 2. Compound **6** was synthesized by a chain extension reaction of 1-octyne.[23] It is interesting that two equivalent of n-butyl lithium will react with 1-octyne to form a 1,3-dilithiooctyne intermediate, which will then react with 1-bromooctane on the more reactive 3-position to give compound **6** after acid treatment and purification. Alkynylmagnesium chloride was generated *in situ* from **6** by reacting with isopropylmagnesium chloride. It reacted with benzo[1,2-b:4,5-b′]dithiophene-4,8-dione at 55 °C. After reduction by $SnCl_2$ in hydrochloride solution, dialkynyl substituted intermediate **7** was obtained in 66% yield. Hydrogenation converted the alkynyl side chain to alkyl and trimethylstannyl monomer **9** was obtained by reacting **8** with n-butyl lithium followed with trimethyltin chloride.[21] It is worth to note that this monomer has a very similar structure as another BDT monomer reported by Yu′s group, where a branched alkoxy group are used instead.[17] It has been reported that the replacement of alkoxy with alkyl group will reduce the electron donating effect and lower the HOMO energy level of the resulted polymers.[21]

Polymers **P1** and **P2** were synthesized *via* Stille coupling reaction as shown in Scheme 3, where BT or FBT were used as electron deficient units and BDT was used as electron rich unit. Both polymers were carefully purified by extracting with acetone

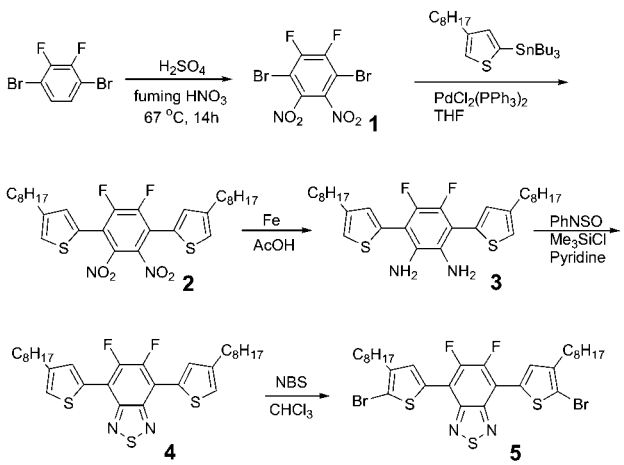

Scheme 1 Synthesis of FBT monomer.

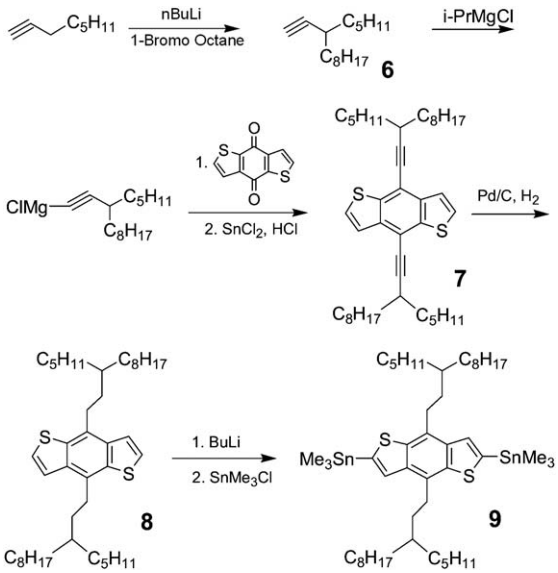

Scheme 2 Synthesis of BDT monomer.

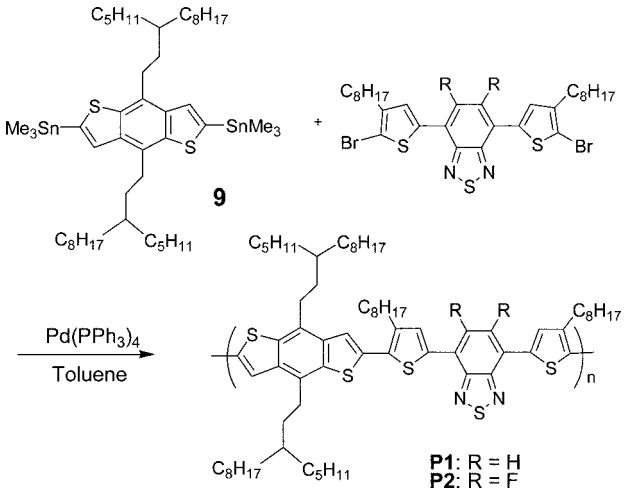

Scheme 3 Preparation of conjugated polymers **P1** and **P2**.

and then hexanes to remove oligmers and other small molecular part, and GPC analysis showed high molecular weight polymers were obtained (Table 1). **P1** can dissolve in chlorobenzene and o-dichlorobenzene at room temperature while **P2** can only dissolve in these solvents at elevated temperature.

2.2. Optical and electrochemical properties

The normalized UV-visible absorption spectra of the chlorobenzene solution and the thin film of polymers **P1** and **P2** are shown in Fig. 1. Both polymers show very similar absorption bands in chlorobenzene solution with a major absorption peak at 558 nm for **P1** and 554 nm for **P2**. This band can be assigned to the intra molecular charge transfer interaction between electron rich and deficient units. The other band in short-wavelength near 400 nm can be assigned to 4,7-dithien-2-yl-2,1,3-benzothiadiazole (DTBT) units, which was often observed in DTBT containing conjugated polymers.[3,5] In the solid state, the main absorption peak becomes broader and the maximum shifts toward longer wavelength at 615 nm for **P1** and 622 nm for **P2**. This large red shift of ~60 nm from solution to solid state means more coplanar structure and stronger inter chain π–π stacking in the solid state. It is interesting that a shoulder peak appeared near 680 nm for **P1** but not for **P2**.

The HOMO and LUMO energy levels of these two polymers were investigated by cyclic voltammetry (Fig. 2). The onset potentials of the first oxidation wave of **P1** and **P2** appeared at 0.92 and 1.10 V, corresponding to HOMO energy levels of 5.30 and 5.48 eV respectively. As expected, this indicated that the introduction of two fluorine atoms on the conjugated backbone

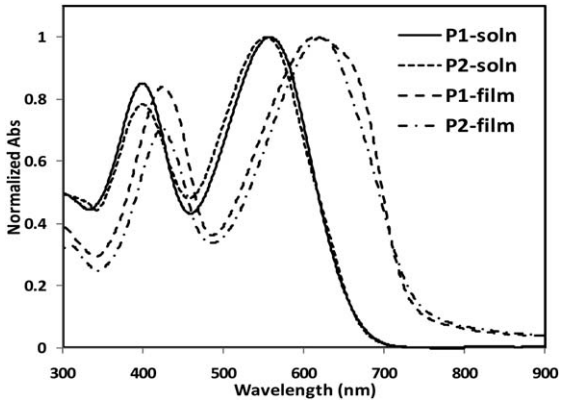

Fig. 1 UV absorption spectra of **P1** and **P2** in dilute chlorobenzene solution (~1.0×10^{-5} $M^{-1}cm^{-1}$) at 50 °C or as a film at RT.

can substantially lower the HOMO energy level of the polymer by 0.18 eV. This fluorine effect was less significant in another fluorinated polymer where only one fluorine atom was attached to each repeating unit of the polymer backbone.[17] Since the first reduction wave of the polymers was hard to determine, the LUMO energy levels were then estimated from the optical band gap and the relative data were summarized in Table 1. It is interesting that the fluorine substitution does not apparently change the UV absorption and band gap, but lowers HOMO energy level. This will lead to an improved V_{oc} for the polymer solar cell devices and better environmental stability of the material.

2.3. Thermal properties and X-ray diffraction (XRD)

The thermal properties of these polymers were studied by differential scanning colorimetry (DSC) and thermal gravimetric analysis (TGA) (Fig. 3). Both **P1** and **P2** showed a broad and strong melting peak at 247 and 284 °C respectively, but no discernible glass transition. A corresponding crystallization peak was also observed for both polymers in the cooling scan with the crystallizing temperature very close to the melting temperature, indicating both polymers have a strong crystallization capability. The thermal decomposition temperatures (2% weight loss) of **P1** and **P2** are 403 °C and 408 °C respectively, showing good thermal stability for optoelectronic devices.

To characterize the crystal structures of these polymers in thin film, XRD studies were carried out and the curves are shown in Fig. 4. The results indicate a lamellar crystal structure for both polymers.[24] A broad peak appeared at 2θ of 6.95° and 6.53° for **P1** and **P2**, corresponding to an inter-layer spacing of 14.8 and 15.7 Å respectively. **P1** showed one broad π–π stacking peak at

Table 1 Polymer characterization

	M_n[a] (kDa)	PDI[a]	Soln λ_{max}[b] abs (nm)	Film λ_{max} abs (nm)	$E_g$opt[c] (eV)	E_{ox}^{onset}[d](V)	LUMO[e](eV)	HOMO[f](eV)
P1	16.2	1.58	399, 558	424, 615	1.60	0.92	3.70	5.30
P2	27.8	2.57	400, 554	424, 622	1.56	1.10	3.92	5.48

[a] Number average molecular weight and polydispersity index (GPC *vs.* polystyrene standards in chlorobenzene). [b] Solution absorption in chlorobenzene. [c] Optical energy gap estimated from the onset of UV curve measured in thin film. [d] CV measurements of thin films in 0.1 M Bu_4NPF_6/CH_3CN solution *vs.* Ag. [e] Estimated from LUMO = HOMO − E_g^{opt}. [f] Estimated from HOMO = E_{ox}^{on} + 4.38 eV.

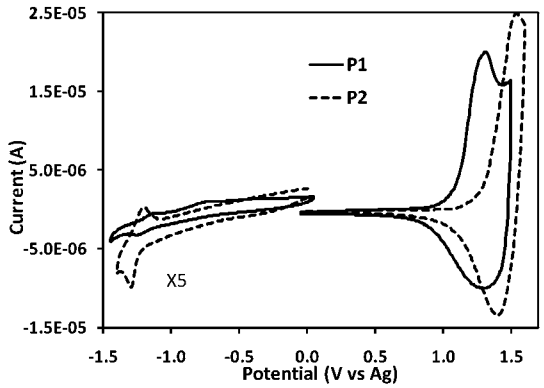

Fig. 2 Cyclic voltammogram of **P1** and **P2** films coated on a platinum electrode in 0.1 M Bu_4NPF_6/CH_3CN solution at RT.

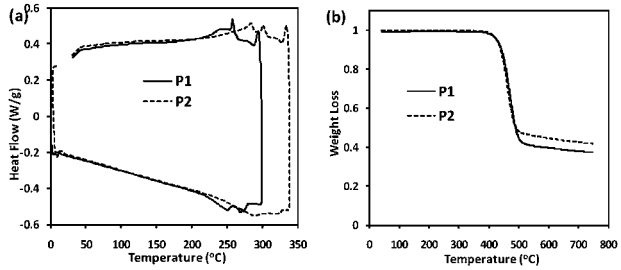

Fig. 3 (a) DSC and (b) TGA curve of **P1** and **P2** with a heating rate of 10 °C min^{-1} in nitrogen.

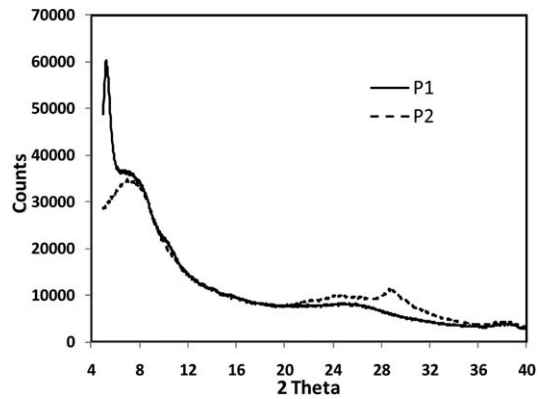

Fig. 4 XRD spectra of **P1** and **P2** thin films.

2θ of 25.2° (4.1 Å), while **P2** showed a broad peak at 23.9° (4.32 Å) and a more strong and narrow peak at 28.3°, corresponding to a very small π–π stacking distance of 3.66 Å. We propose that there is stronger interchain interaction in the fluorinated polymer **P2** than in **P1**, as **P2** shows poorer solubility, higher melting point and closer stacking distance.

2.4. Field effect transistor characterization and photovoltaic performance

As the performance of organic optoelectronic materials for transistor or photovoltaic applications is closely related to their charge carrier mobility, we fabricated bottom-contact organic thin-film transistors (OTFT) to measure the field-effect mobility of these polymers. Fig. 5 shows representative *I–V* characteristics of these devices fabricated from **P1** and **P2**. Both polymers displayed a well-defined saturation region with p-channel transport (h^+) mobility of 2.12×10^{-4} cm^2/Vs for **P1** and 4.88×10^{-5} cm^2/Vs for **P2** respectively. To our surprise, **P2** has a lower hole mobility, although it has a higher crystallization capability than **P1**. We do not have a clear explanation for this phenomenon. It might be related to the orientation of the crystal structure relative to the substrate. In addition, the relative poor film quality of polymer **P2** due to its low solubility may also influence the charge transfer. This issue could be improved by adjusting the processing conditions such as the solvent, temperature, spin speed, annealing and so on.

Polymer solar cells were fabricated from **P1** or **P2** and (6,6)-phenyl-C_{71}-butyric acid methyl ester ($PC_{71}BM$) with a general device structure of ITO/PEDOT:PSS/Polymer: $PC_{71}BM$/LiF/Al. Different polymer to fullerene weight ratio, solvents and processing temperature are tested to optimize the device performance. Fig. 6a showed typical current density-voltage (J-V) curves and the devices performance data were summarized in Table 2. Device fabricated from a blend of **P1** with $PC_{71}BM$ at 1/2 weight ratio gave a V_{oc} of 0.69 V, a short-circuit current density (J_{sc}) of 6.15 mA cm^{-2}, a modest fill factor (FF) of 44.3% and a PCE of 1.88%. The device from **P2** with $PC_{71}BM$ at 1/1 weight ratio gives a better result with a similar V_{oc} of 0.69 V, a higher J_{sc} of 8.89 mA cm^{-2} and an improved FF of 55.4%. The PCE thus reached 3.4%. It should be noted that the best device for **P1** is fabricated from *o*-dichlorobenzene solution with 2.5% DIO as an additive at 70 °C while the blend of **P2** and $PC_{71}BM$ has to be spin-coated from 1,2,4-trichlorobenzene solution at 90 °C. It is important that different solvents and processing temperature should be used to get optimized performance. We noted that the devices from **P1** and **P2** show similar V_{oc} although there is a big difference between their HOMO energy levels (0.18 eV).[16] This is tentatively explained by the decreased surface energy of fluorinated polymer. The lower surface energy of the fluorinated polymer enhanced the tendency of the polymer to

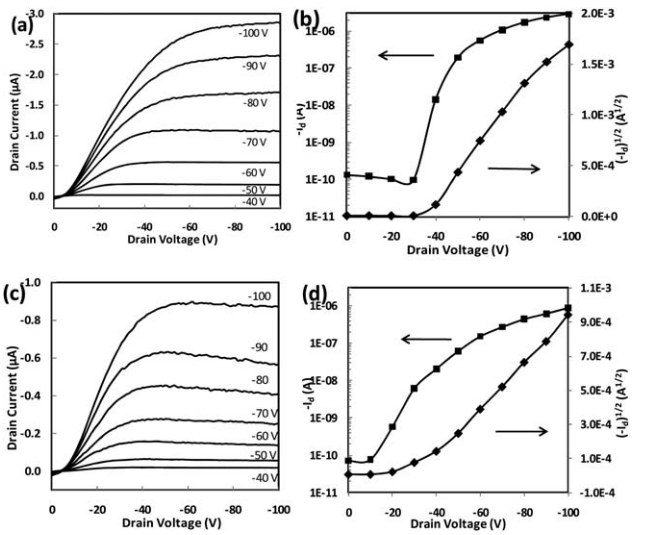

Fig. 5 Output characteristics of p-type OFET devices of **P1** (a, b) and **P2** (c, d) tested in glove box.

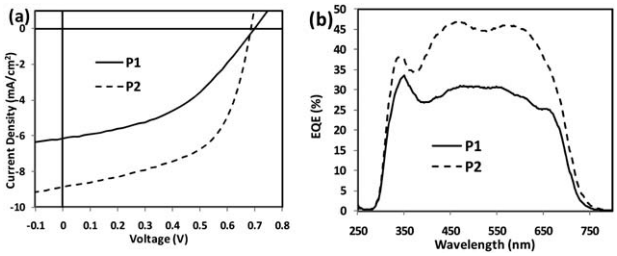

Fig. 6 (a) J-V curve of **P1**:$PC_{71}BM$ (weight ratio 1 : 2) and **P2**:$PC_{71}BM$ (weight ratio 1 : 1) BHJ solar cells under illumination of AM 1.5G, 100 mW cm^{-2}, (b) EQE spectra of these BHJ solar cells.

migrate to the air/film interface during spin coating,[25] resulting in the relative enrichment of the polymer at the top of the active layer. This kind of structure is not beneficial for charge transport to corresponding electrodes and could lower the V_{oc} of the devices because of the accumulation of space charge. However, this fluorinated polymer may be used in an inverted structure where high concentration of polymer on top layer will benefit.[25] As shown in Fig. 6b, external quantum efficiency (EQE) curves of these devices were tested which cover 300 nm to 700 nm range. Devices of **P2** showed a higher efficiency (~45%) than **P1** (~30%), and the integrated J_{sc} from EQE data agrees well with the data from J-V curves (see Table 2).

2.5. Atomic force microscopy (AFM) images and stability characterization

We then studied the surface morphological structure of the polymer/$PC_{71}BM$ blend film using tapping mode AFM and the images are shown in Fig. 7. The phase image of the film from **P1** with $PC_{71}BM$ (Fig. 7c) showed obscure domains without clear phase segregation, this may explain the modest FF of 44.3% obtained from this device. However, the film from **P2** and $PC_{71}BM$ has a more clear structure which shows bright domains with the size of ~20 nm. This domain size is desired for better charge separation, and thus agrees with the improved FF of 55%. It should be noted that the phase image scale for **P2** (0–100°) is much larger than the one for **P1** (0–30°). The bright spots in Fig. 7d can be assigned to the crystalline domains of fluorinated polymer **P2** due to decreased surface energy,[26] and the detection of polymer **P2** on the top layer of the film also partially support our previous assumption on the accumulation of the fluorinated polymer on air/film interface.

Polymer thin films (~40 nm) were prepared by spin coating *o*-dichlorobenzene solution on glass substrate and the stability of the polymer thin films in air was investigated by UV-vis

Table 2 Summary of device performance

	Ratio[a]	Solvent	J_{sc}[d](mA cm^{-2})	V_{oc} (V)	FF (%)	PCE[d] (%)
P1	1 : 2	DCB[b]	6.15 (5.89)	0.69	44.3	1.88 (1.80)
P2	1 : 1	TCB[c]	8.89 (8.83)	0.69	55.4	3.40 (3.38)

[a] Polymer/$PC_{71}BM$ weight raio. [b] Containing 1.8-diiodooctane (2.5% volume ratio) as additives. [c] TCB = 1,2,4-trichlorobenzene. [d] Data calculated from EQE spectrum are shown in bracket.

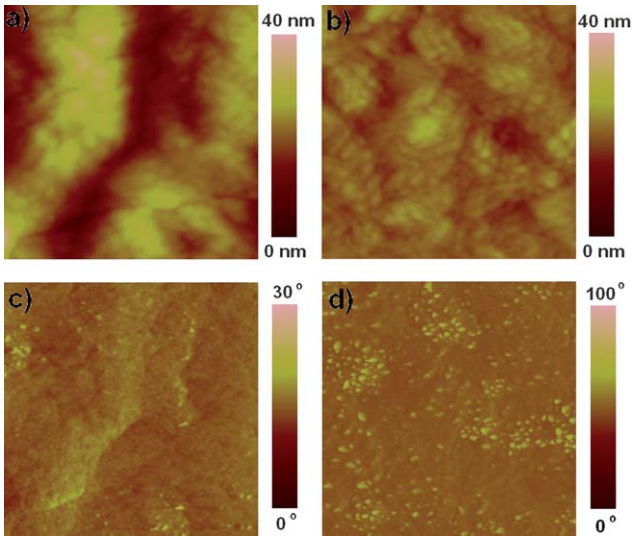

Fig. 7 AFM topography (a, b) and phase (c, d) images of **P1**:$PC_{71}BM$ (1 : 2, w/w) (a, c) and **P2**:$PC_{71}BM$ (1 : 1, w/w) (b, d) films. The scan size of the image is 1μm × 1μm.

spectrum. The absorption spectra of these thin films were monitored over time while keeping the films under ambient condition. It was reported that oxygen and water can diffuse into the active layer of a polymer solar cell and cause photo-oxidative bleaching under ambient condition and continuous illumination.[27] The degree of this oxidative reaction for the donor polymer is closely related to the position of its HOMO energy level. Fig. 8a showed that the maximum absorption of **P1** film decreased by 27% and blue shift from 615 nm to 586 nm after exposure to air and ambient light for 312 h, meaning dramatic decreasing of the number of original polymer chains and shortening of the conjugation length. However, after the same exposure, the maximum absorption peak of polymer **P2** only decreased by 17% and the position retained at 620 nm. This result demonstrates the improved stability of this series of polymer by fluorine substitution and agrees well with the lowered HOMO energy level from CV data.

3. Conclusions

A new fluorinated benzothiadiazole monomer, FBT is designed and synthesized. Two alternating conjugated polymers **P1** and **P2** are prepared based on electron deficient BT or FBT and electron rich BDT monomers. The optical, electrochemical and thermal studies of these two polymers show that the fluorine substitution will not change the UV absorption, but will significantly lower the HOMO energy level. However, this does not result in a higher V_{oc} in the polymer solar cell devices. This phenomenon is believed to be associated with the enrichment of **P2** on the top surface of the active layer due to the low surface energy of the polymer as observed by AFM. TFT characterization shows **P2** has lower hole mobility, but this drawback may be compensated by the better domain structure formed in the device with enhanced charge separation and transfer, thus better FF and higher PCE are observed from the **P2** devices. Finally, the improved environmental stability of the fluorinated polymer is

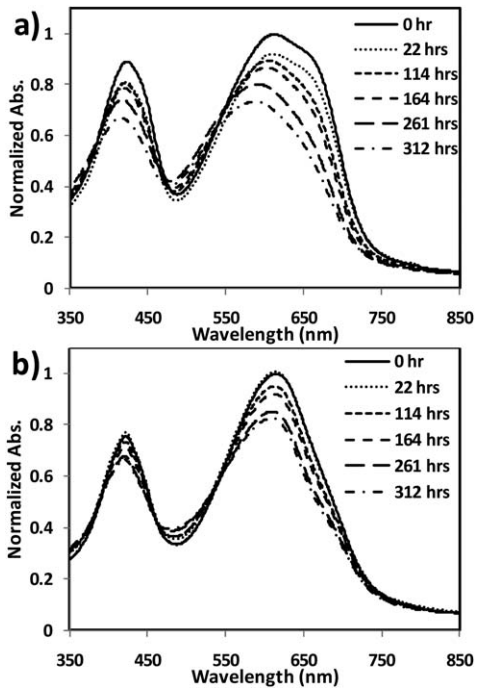

Fig. 8 Change of the UV absorption spectra of thin films of **P1** (a) and **P2** (b) with time in ambient conditions.

confirmed by the UV study of polymer thin films which are aged in air under ambient light.

4. Experimental

4.1. General characterization methods

NMR spectra were recorded in $CDCl_3$ or *o*-dichlorobenzene-d_4 using a Varian Unity Inova spectrometer at a resonance frequency of 399.96 MHz for ^1H, 376.29 MHz for ^{19}F, and 100.58 MHz for ^{13}C. ^1H and ^{19}F NMR spectra were obtained using a 5 mm indirect detection probe. A 5 mm broadband probe was used for acquiring ^{13}C NMR spectra. $CFCl_3$ was used as an internal standard (0 ppm) for the ^{19}F NMR measurements. Gel permeation chromatography (GPC) (Waters Breeze HPLC system with 1525 Binary HPLC Pump and 2414 Differential Refractometer) was used for measuring the molecular weight and polydispersity index at 40 °C. Chlorobenzene was used as eluent and commercial polystyrenes were used as standard. UV-vis spectra were measured using a Varian Cary 5000 Spectrometer. The differential scanning calorimetry (DSC) analysis was performed under a nitrogen atmosphere (50 mL min^{-1}) using a TA Instruments DSC 2920 at a heating rate of 10 °C min^{-1}, calibrated with the melting transition of indium. The thermal gravimetric analysis (TGA) was performed using a TA Instruments TGA 2950 at a heating rate of 10 °C min^{-1} under a nitrogen atmosphere (60 mL min^{-1}). MS data were obtained using a Prince capillary electrophoresis system coupled to an API3000 mass spectrometer *via* a microspray interface. A sheath solution of 1 μL min^{-1} 2-propanol/methanol (2 : 1) was used, with 30 mM ammonium acetate dichloromethane–methanol (3 : 1) as the running buffer. Cyclic voltammetry (CV) measurements were carried out under argon in a three-electrode cell using 0.1 M Bu_4NPF_6 in anhydrous CH_3CN as the supporting electrolyte. The polymers were coated on the platinum-working electrode. The CV curves were recorded referenced to an Ag quasi-reference electrode, which was calibrated using a ferrocene/ferrocenium (Fc/Fc^+) redox couple (4.8 eV below the vacuum level) as an external standard. The $E_{1/2}$ of the Fc/Fc^+ redox couple was found to be 0.42 V *vs.* the Ag quasi-reference electrode. Therefore, the HOMO energy level of the copolymers can be estimated using the empirical equation $E_{HOMO} = E_{ox}^{on} + 4.38$ eV, where E_{ox}^{on} stands for the onset potentials for oxidation relative to the Ag quasi-reference electrode. X-ray diffraction (XRD) spectrum was obtained with a Bruker AXS D8 Advance instrument with Co Kα^1 radiation ($\lambda = 1.789$ Å).

4.2. Synthesis

Materials. 1,4-dibromo-2,3-difluorobenzene,[18] 4,7-bis(5-bromo-4-dioctyl-2-thienyl)-2,1,3-benzothiadiazole,[9] and benzo [1,2-b:4,5-b′] dithiophene-4,8-dione[28] were synthesized according to literature.

1,4-Dibromo-2,3-difluoro-5,6-dinitrobenzene (1). Fuming nitric acid (100 mL, 90%) was added slowly to 100 mL of concentrated sulfuric acid solution at 5 °C in an ice water bath. Then 1,4-dibromo-2,3-difluorobenzene (20 g, 74 mmol) was added drop wise. After stirring at room temperature (RT) for 4 h, the solution was stirred at 67 °C for 14 h. The resulting mixture was poured into 1400 mL of ice water and the formed yellow precipitate was collected by filtration. Then the crude product was purified by column chromatography on silica gel with hexanes/dichloromethane (4/1 to 3/1 volume ratio). The third fraction provided 8.3 g white solid (yield 31%) as product, ^{19}F NMR ($CDCl_3$) δ: −114.3 (s, 2F); ^{13}C NMR ($CDCl_3$) δ: 151.2 (d), 148.6 (d), 141.4, 105.7. Mp 121.2 °C. HRMS EI calcd for $C_6Br_2F_2N_2O_4$ 359.81929, found 359.81862.

1,4-Bis(4-octyl-2-thienyl)-2,3-difluoro-5,6-dinitrobenzene (2). Compound **1** (0.362 g, 1.00 mmol), 2-tributylstannyl-4-octylthiophene (0.970 g, 2.20 mmol) and dichlorobis-(triphenylphosphine) palladium (0.028 g, 0.040 mmol) were put in a flask, which was purged with argon under vacuum for three times before 12 mL of dry THF was added. The solution was refluxed under argon for 54 h. Then the solvent was removed and the residue was purified by column chromatograph with hexanes/dichloromethane (4/1 volume ratio) to give 0.35 g yellow powder (Yield: 60%). ^1H NMR ($CDCl_3$) δ: 7.20 (d, 2H), 7.03 (d, 2H), 2.62 (t, 4H), 1.61 (m, 4H), 1.28 (t, 20H), 0.88 (t, 6H); ^{19}F NMR ($CDCl_3$) δ: −126.6; ^{13}C NMR ($CDCl_3$) δ: 150.2 (d), 147.6 (d), 144.3, 139.3, 131.8, 125.1, 124.7, 119.8, 31.8, 30.3, 30.2, 29.4, 29.2, 29.1, 22.7, 14.1. MS (*m*/*z*): observed: 593.2, calculated: 593.2 for $[M - H]^+$.

1,4-Bis(4-octyl-2-thienyl)-2,3-difluoro-5,6-diaminobenzene (3). To a mixture of compound **2** (0.35 g, 0.59 mmol) and iron powder (0.40 g, 7.1 mmol) was added with acetic acid (12 mL). The mixture was stirred at 45 °C for 4 h before poured into 25 mL of cold 5% NaOH solution. The solution was extracted with ether and the organic phase was washed with 5% $NaHCO_3$ solution for 5 times. After dried over $MgSO_4$, the solvent was

removed and the product was purified by column chromatograph with 2/3 hexanes/dichloromethane to give pale solid (yield: 73%). ^{1}H NMR ($CDCl_3$) δ: 7.07 (d, 2H), 6.98 (d, 2H), 3.62 (s, 4H), 2.64 (t, 4H), 1.65 (m, 4H), 1.32 (m, 20H), 0.88 (t, 6H); ^{19}F NMR ($CDCl_3$) δ: −150.3; ^{13}C NMR ($CDCl_3$) δ: 143.8, 143.4 (d), 141.0 (d), 131.1, 130.3, 129.3, 121.8, 111.2, 31.9, 30.5, 30.4, 29.4, 29.3, 29.2, 22.7, 14.1. MS (*m*/*z*): observed: 532.9, calculated: 533.2 for $[M - H]^+$.

5,6-Difluoro-4,7-bis(4-octyl-2-thienyl)-2,1,3-benzothiadiazole (4). To a solution of compound **3** (2.13 g, 4.0 mmol) in dry pyridine (40 mL), N-thionylaniline (0.90 g, 8.0 mmol) and trimethylsilyl chloride (0.91 g, 7.2 mmol) were added under argon. Then the solution was stirred at 80 °C for 16 h before was poured into ice water, the resulted solid was filtered and washed with ethanol to give 2.1 g yellow solid (yield: 94%). ^{1}H NMR ($CDCl_3$) δ: 8.11 (d, 2H), 7.20 (d, 2H), 2.71 (t, 4H), 1.68 (m, 4H), 1.32 (m, 20H), 0.88 (t, 6H); ^{19}F NMR ($CDCl_3$) δ: −128.7; ^{13}C NMR ($CDCl_3$) δ: 151.0 (d), 148.9, 148.5 (d), 132.2, 131.2, 123.9, 111.7, 31.9, 30.6, 30.5, 29.4, 29.3, 29.2, 22.7, 14.1. Mp 94.4 °C. MS (*m*/*z*): observed: 560.9, calculated: 561.2 for $[M - H]^+$.

4,7-Bis(5-bromo-4-octyl-2-thienyl)-5,6-difluoro-2,1,3-benzothiadiazole (5). Compound **4** (1.88 g, 3.35 mmol) and NBS (1.19 g, 6.70 mmol) were dissolved in 70 mL chloroform before 0.17 g silica gel was added. After stirring at RT for 3.5 h, the solvent was removed and residue was purified by column chromatograph with hexanes/chloroform (1/1 volume ratio) to give 2.37 g yellow solid (yield: 98%). ^{1}H NMR ($CDCl_3$) δ: 7.96 (s, 2H), 2.65 (t, 4H), 1.66 (m, 4H), 1.32 (m, 20H), 0.87 (t, 6H); ^{19}F NMR ($CDCl_3$) δ: −128.6; ^{13}C NMR ($CDCl_3$) δ: 151.0 (d), 148.4, 148.2 (d), 142.6, 131.7, 131.2, 114.4, 111.0, 31.9, 29.8, 29.6, 29.4, 29.3, 22.7, 14.1. Mp 96.4 °C. MS (*m*/*z*): observed: 718.6, calculated: 718.0 for $[M - H]^+$.

3-Pentyl undec-1-yne (6). In a 500 mL flask purged with argon, dry hexane (150 mL) and 1-octyne (16.5 g, 0.15 mol) was added. Then n-BuLi (2.5M in hexane, 132 mL, 0.33 mol) was dropwise added in a dry ice/acetone bath. After stirring at −78 °C for 30 min, the solution was warmed up to −42 °C using an acetonitrile/dry ice bath for 1 h. Freshly distilled 1-bromooctane (29.0 g, 0.15 mol) was added and the mixture was allowed to slowly warm up to RT overnight. HCl (6 M, 150 mL) was slowly added in an ice water bath. The organic phase was separated and washed with water, dried over $MgSO_4$. The product was purified by vacuum distillation to give slightly yellowish oil (15 g, yield: 45%). ^{1}H NMR ($CDCl_3$) δ: 2.30 (m, 1H), 2.03 (d, 2H), 1.2–1.5 (m, 22H), 0.9 (m, 6H). HRMS EI calcd for $C_{16}H_{34}$ 226.2661, found 226.2650 (M + 4H).

4,8-Di(3-pentylundecyn)benzo[1,2-b:4,5-b′]dithiophene (7). To a solution of compound **6** (3.5 g, 13.6 mmol) in THF (4 mL), isopropylmagnesium chloride (2 M in THF, 5.1 mL, 12.0 mmol) was dropwise added. The solution was stirred for 90 min at 55 °C before benzo [1,2-b:4,5-b′] dithiophene-4,8-dione (0.5 g, 2.27 mmol) was added. After 60 min, $SnCl_2$ solution (3.5 g in 8 mL 10% HCl) was slowly added. The solution was stirred for another 60 min at 65 °C before was poured into water and extracted with hexane. The product was purified by column chromatograph to give white powder (0.94 g, yield: 66%). ^{1}H NMR ($CDCl_3$) δ: 7.55 (d, 2H), 7.48 (d, 2H), 2.74 (m, 2H), 1.2–1.8 (m, 44H), 0.9 (m, 12H).

4,8-Di(3-pentylundecyl)benzo[1,2-b:4,5-b′]dithiophene (8). Compound **7** (2.0 g, 3.17 mmol) and Pd/C (0.44 g) was added into a 250 mL flask. After purge with argon, dry THF (80 mL) was added. The mixture was purged with H_2 at a speed of 5 mL min^{-1} for 16 h. The product was purified by column chromatograph with 2% dichloromethane in hexanes to give white solid product (1.62 g, yield: 80%). ^{1}H NMR ($CDCl_3$) δ: 7.44 (s, 4H), 3.12 (m, 4H), 1.73 (m, 4H), 1.5 (m, 2H), 1.2–1.4 (m, 44H), 0.9 (m, 12H).

1,5-Bis(trimethylstannyl)-4,8-di(3-pentylundecyl)benzo-[1,2-b:4,5-b′]dithiophene (9). Compound **8** (3.1 g, 4.8 mmol) was dissolved in dry THF (45 mL) in an argon purged flask. The solution was cooled to −78 °C before n-BuLi (2.5 M in THF, 4.7 mL, 11.7 mmol) was added dropwise. After stirring at −78 °C for 30 min, the temperature of the solution was raised to RT for 30 min. Then the solution was cooled to −78 °C again and trimethyltin chloride (1 M in hexane, 13.6 mL, 13.6 mmol) was added. The solution was allowed to warm to RT overnight before added with hexane and washed with water. The product was purified by recrystallization in 2-propanol to get white needles (3.3 g, yield: 71%). ^{1}H NMR ($CDCl_3$) δ: 7.48 (s, 2H), 3.14 (m, 4H), 1.75 (m, 4H), 1.50 (m, 2H), 1.2–1.4 (m, 44H), 0.88 (m, 12H). ^{13}C NMR (Acetone-d_6) δ: 206.0, 142.3, 141.5, 137.8, 130.5, 128.3, 38.3, 34.4, 33.6, 33.1, 32.7, 30.9, 30.8, 30.6, 30.2, 27.6, 27.3, 23.5, 23.4, 14.5, 14.4, −8.3. Mp 42.5 °C.

General procedure for Stille reaction. The BT monomer, 4,7-bis(5-bromo-4-dioctyl-2-thienyl)-2,1,3-benzothiadiazole (0.205 g, 0.300 mmol) or monomer **5** (0.216 g, 0.300 mmol) and compound 9 (0.289 g, 0.300 mmol) were added into a 25 mL flask equipped with a condenser. The system was purged with argon before $Pd(PPh_3)_4$ (0.028 g, 0.040 mmol) was added in a dry box. Toluene (8 mL) was added and the solution was refluxed for 48 h. The polymer solution was precipitated into methanol, and the obtained powder was Soxhlet extracted with acetone and then hexanes to remove oligmers and small molecular part. Then the product was collected with toluene to give deep purple shining film. **P1** (0.20 g, yield: 57%). ^{1}H NMR (1,2-dichlorobenzene-d_4, 60 °C) δ: 8.26 (s, 2H), 7.81 (s, 2H), 7.79 (s, 2H), 3.30 (br, 4H), 3.15 (br, 4H), 1.96, (br, 8H), 1.2–1.8 (br, 66H), 0.90 (br, 18H). GPC analysis: M_n = 16200 g mol^{-1}, M_w = 25600 g mol^{-1}, PDI = 1.58. **P2** (0.13 g, yield: 36%). ^{1}H NMR (1,2-dichlorobenzene-d_4, 60 °C) δ: 8.41 (s, 2H), 7.82 (s, 2H), 3.32 (br, 4H) 3.17 (br, 4H), 1.96 (br, 8H), 1.2–1.8 (br, 66H), 0.90 (br, 18H); ^{19}F NMR (*o*-DCB-d_4, 60 °C) δ: −127.8. GPC analysis: M_n = 27800 g mol^{-1}, M_w = 71400 g mol^{-1}, PDI = 2.57.

4.3. Device fabrication and testing

Bottom-contact thin film transistors were fabricated by spin-coating **P1** and **P2** in *o*-dichlorobenzene solution at 60 °C on a heavily doped n-Si wafer with an overlayer of SiO_2 (230 nm, Ci = 15 nF/cm^2). Then gold source and drain electrodes were sputtered on the substrate prior to the deposition of polymer

film. The transistor channel length and width are 20 μm and 10 mm, respectively. The current–voltage (J-V) characteristics were measured with a computer-controlled semiconductor parameter analyzer (HP4145A) in a N_2 glove box. The hole mobility was deduced from the saturation regime of the J-V characteristics.

Polymer solar cells were fabricated with a general structure of ITO/PEDOT:PSS/Polymer:$PC_{71}BM$/LiF/Al. Patterned ITO glass substrates were cleaned with detergent before sonicated in CMOS grade acetone and isopropanol for 15 min. The organic residue was further removed by treating with UV-ozone for 10 min. Then a thin layer of PEDOT:PSS (Clevios P, H. C. Starck, 45 nm) was spin-coated and dried for 1 h at 120 °C. Polymer **P1** or **P2** and $PC_{71}BM$ (ADS) (1 : 2 weight ratio) were dissolved in o-dichlorobenzene containing 2.5% (v/v) diiodooctane or 1,2,4-trichlorobenzene at 80 °C to form a mixture solution. The solution was filtered and spin-coated on the top of PEDOT:PSS layer. The border of the PEDOT:PSS layer and active layer was mechanically removed before 1.0 nm of LiF and 100 nm Al layer were thermally evaporated through a shadow mask at a pressure of 5×10^{-7} mbar in a Boc Edwards Auto 500 System. The active area is 49 mm^2.

The current–voltage (J-V) characteristics were measured with a Keithley 2400 digital source meter under simulated air mass (AM) 1.5 solar irradiation of 100 mW cm^{-2} (Sciencetech Inc., SF150). The light intensity was calibrated with a power meter (Gentec Solo PE Laser Power & Energy Meter). The external quantum efficiency (EQE) was performed using a Jobin-Yvon Triax 180 spectrometer, a Jobin-Yvon xenon light source, a Merlin lock-in amplifier, a calibrated Si UV detector, and an SR 570 low noise current amplifier.

Notes and references

1 B. C. Thompson and J. M. J. Fréchet, *Angew. Chem., Int. Ed.*, 2008, **47**, 58; G. D. Dennler, M. C. Scharber and C. J. Brabec, *Adv. Mater.*, 2009, **21**, 1323; Y.-J. Cheng, S.-H. Yang and C.-S. Hsu, *Chem. Rev.*, 2009, **109**, 5868; S. Günes, H. Neugebauer and N. S. Sariciftci, *Chem. Rev.*, 2007, **107**, 1324.

2 G. Yu, J. Gao, J. C. Hummelen, F. Wudl and A. J. Heeger, *Science*, 1995, **270**, 1789; J. J. M. Halls, C. A. Walsh, N. C. Greenham, E. A. Marseglia, R. H. Friend, S. C. Moratti and A. B. Holmes, *Nature*, 1995, **376**, 498.

3 M. Svensson, F. Zhang, S. C. Veenstra, W. J. H. Verhees, J. C. Hummelen, J. M. Kroon, O. Inganäs and M. R. Andersson, *Adv. Mater.*, 2003, **15**, 988; M.-H. Chen, J. Hou, Z. Hong, G. Yang, S. Sista, L.-M. Chen and Y. Yang, *Adv. Mater.*, 2009, **21**, 4238.

4 D. Mühlbacher, M. Scharber, M. Morana, Z. Zhu, D. Waller, R. Gaudiana and C. Brabec, *Adv. Mater.*, 2006, **18**, 2884; R. C. Coffin, J. Peet, J. Rogers and G. C. Bazan, *Nat. Chem.*, 2009, **1**, 657.

5 N. Blouin, A. Michaud and M. Leclerc, *Adv. Mater.*, 2007, **19**, 2295; N. Blouin, A. Michaud, D. Gendron, S. Wakim, E. Blair, R. Neagu-Plesu, M. Belletête, G. Durocher, Y. Tao and M. Leclerc, *J. Am. Chem. Soc.*, 2008, **130**, 732.

6 J. Hou, M.-H. Park, S. Zhang, Y. Yao, L.-M. Chen, J.-H. Li and Y. Yang, *Macromolecules*, 2008, **41**, 6012.

7 E. Zhou, M. Nakamura, T. Nishizawa, Y. Zhang, Q. Wei, K. Tajima, C. Yang and K. Hashimoto, *Macromolecules*, 2008, **41**, 8302.

8 J. Hou, H.-Y. Chen, S. Zhang, G. Li and Y. Yang, *J. Am. Chem. Soc.*, 2008, **130**, 16144.

9 J. Lu, F. Liang, N. Drolet, J. Ding, Y. Tao and R. Movileanu, *Chem. Commun.*, 2008, 5315.

10 Q. Zheng, B. J. Sun, J. Jung and H. E. Katz, *J. Am. Chem. Soc.*, 2010, **132**, 5394.

11 S. H. Park, A. Roy, S. Beaupre, S. Cho, N. Coates, J. S. Moon, D. Moses, M. Leclerc, K. Lee and A. J. Heeger, *Nat. Photonics*, 2009, **3**, 297.

12 R. Qin, W. Li, C. Li, C. Du, C. Veit, H.-F. Schleiermacher, M. Andersson, Z. Bo, Z. Liu, O. Inganäs, U. Wuerfel and F. Zhang, *J. Am. Chem. Soc.*, 2009, **131**, 14612.

13 C. Kitamura, S. Tanaka and Y. Yamashita, *Chem. Mater.*, 1996, **8**, 570.

14 E. Bundgaard and F. C. Krebs, *Macromolecules*, 2006, **39**, 2823; A. P. Zoombelt, M. Fonrodona, M. M. Wienk, A. B. Sieval, J. C. Hummelen and R. A. J. Janssen, *Org. Lett.*, 2009, **11**, 903.

15 F. Babudri, G. M. Farinola, F. Naso and R. Ragni, *Chem. Commun.*, 2007, 1003.

16 M. C. Scharber, D. Mühlbacher, M. Koppe, P. Denk, C. Waldauf, A. J. Heeger and C. J. Brabec, *Adv. Mater.*, 2006, **18**, 789.

17 Y. Liang, D. Feng, Y. Wu, S.-T. Tsai, G. Li, C. Ray and L. Yu, *J. Am. Chem. Soc.*, 2009, **131**, 7792; H.-Y. Chen, J. Hou, S. Zhang, Y. Liang, G. Yang, Y. Yang, L. Yu, Y. Wu and G. Li, *Nat. Photonics*, 2009, **3**, 650.

18 J. P. Dunn, T. R. Elworthy, D. Stefanidis and Z. K. Sweeney, WO 010545 A1, 2006.

19 Y. Yamashita, K. Ono, M. Tomura and S. Tanaka, *Tetrahedron*, 1997, **53**, 10169.

20 Z. Li, J. Ding, N. Song, J. Lu and Y. Tao, *J. Am. Chem. Soc.*, 2010, **132**, 13160.

21 H. Pan, Y. Li, Y. Wu, P. Liu, B. S. Ong, S. Zhu and G. Xu, *J. Am. Chem. Soc.*, 2007, **129**, 4112; H. Pan, Y. Li, Y. Wu, P. Liu, B. S. Ong, S. Zhu and G. Xu, *Chem. Mater.*, 2006, **18**, 3237; J. Hou, H.-Y. Chen, S. Zhang, R. I. Chen, Y. Yang, Y. Wu and G. Li, *J. Am. Chem. Soc.*, 2009, **131**, 15586.

22 S. C. Price, A. C. Stuart and W. You, *Macromolecules*, 2010, **43**, 4609.

23 S. Bhanu and F. Scheinmann, *J. Chem. Soc., Perkin Trans. 1*, 1979, 1218.

24 C. Piliego, T. W. Holcombe, J. D. Douglas, C. H. Woo, P. M. Beaujuge and J. M. J. Fréchet, *J. Am. Chem. Soc.*, 2009, **132**, 7595.

25 J. S. Kim, Y. Lee, J. H. Lee, J. H. Park, J. K. Kim and K. Cho, *Adv. Mater.*, 2010, **22**, 1355.

26 L.-M. Chen, Z. Hong, G. Li and Y. Yang, *Adv. Mater.*, 2009, **21**, 1434.

27 M. Jørgensen, K. Norrman and F. C. Krebs, *Sol. Energy Mater. Sol. Cells*, 2008, **92**, 686.

28 P. Beinilirig and G. Koβmehl, *Chem. Ber.*, 1986, **119**, 3198.